

Features in optical absorption and photocurrent spectra of organic solar cells due to organic/organic interface

Yasser A. M. Ismail, Tetsuo Soga, and Takashi Jimbo

Citation: *J. Appl. Phys.* **109**, 103109 (2011); doi: 10.1063/1.3586520

View online: <http://dx.doi.org/10.1063/1.3586520>

View Table of Contents: <http://jap.aip.org/resource/1/JAPIAU/v109/i10>

Published by the [American Institute of Physics](http://www.aip.org).

Related Articles

Towards an optimized all lattice-matched InAlAs/InGaAsP/InGaAs multijunction solar cell with efficiency >50%
Appl. Phys. Lett. **102**, 033901 (2013)

Thin-film-based CdTe photovoltaic module characterization: Measurements and energy prediction improvement
Rev. Sci. Instrum. **84**, 015114 (2013)

Enhanced external quantum efficiency in rectangular single nanowire solar cells
Appl. Phys. Lett. **102**, 021101 (2013)

Modelling of GaAsP/InGaAs/GaAs strain-balanced multiple-quantum well solar cells
J. Appl. Phys. **113**, 024512 (2013)

Ethanol-enriched low-pressure chemical vapor deposition ZnO bilayers: Properties and growth—A potential electrode for thin film solar cells
J. Appl. Phys. **113**, 024908 (2013)

Additional information on J. Appl. Phys.

Journal Homepage: <http://jap.aip.org/>

Journal Information: http://jap.aip.org/about/about_the_journal

Top downloads: http://jap.aip.org/features/most_downloaded

Information for Authors: <http://jap.aip.org/authors>

ADVERTISEMENT



AIP Advances

Now Indexed in Thomson Reuters Databases

Explore AIP's open access journal:

- Rapid publication
- Article-level metrics
- Post-publication rating and commenting

Features in optical absorption and photocurrent spectra of organic solar cells due to organic/organic interface

Yasser A. M. Ismail,^{a)} Tetsuo Soga, and Takashi Jimbo

Department of Frontier Materials, Nagoya Institute of Technology, Gokiso-cho, Showa-ku, Nagoya 466-8555, Japan

(Received 29 June 2010; accepted 5 April 2011; published online 17 May 2011)

We surprisingly found that, organic/organic interface had a direct and pronounced impact on optical absorption and photocurrent spectra of organic solar cell at a favorable wavelength region of the visible solar spectrum. The organic/organic interface was formed as a result of connection between coumarin 6 (C6): [6,6]-phenyl-C₆₁ butyric acid methyl ester (PCBM) blend films and indium-tin oxide (ITO)/poly(3,4-ethylenedioxythiophene) doped with poly(styrene sulfonate) (PEDOT:PSS) electrode. Optical absorption measurement was carried out for ITO/PEDOT:PSS/C6:PCBM films, while external quantum efficiency measurement was carried out for ITO/PEDOT:PSS/C6:PCBM/Al solar cells, with varying C6:PCBM blend concentration. We found that, the C6:PCBM blend in the ITO/PEDOT:PSS/C6:PCBM films had an additional feature in the absorption spectra at the wavelength range of 520–800 nm, at which the C6 dye, PCBM, PEDOT:PSS, and ITO were transparent. An additional feature, also, appeared in photocurrent spectra of the C6:PCBM films in the ITO/PEDOT:PSS/C6:PCBM/Al solar cells at the same wavelength range. The new features in the optical absorption and photocurrent spectra of the investigated solar cells originated, in all probability, due to optically induced sup-band transitions in the C6:PCBM blend films at the interface with ITO/PEDOT:PSS electrode. Thus, the C6:PCBM blend films produced a charge carrier generation interface due to connection with ITO/PEDOT:PSS electrode. As a result of this charge carrier generation interface, the power conversion efficiency of the corresponding solar cell is improved. Taking into consideration these new findings, the high-band-gap organic materials will take more importance as sensitizers in organic optoelectronic applications. © 2011 American Institute of Physics. [doi:10.1063/1.3586520]

I. INTRODUCTION

In recent years, the development of organic solar cells has made significant progress for increasing their power conversion efficiencies.^{1,2} The development has included synthesis of novel organic materials^{3–5} possessing proper properties in solar cell applications, use a sensitizer in solar cell active layer for light harvesting,⁶ use a transporting material in the active layer for increasing charge carrier mobility,⁷ use a new architecture,⁸ etc. There were many attempts for improving solar cell properties through modification of interfaces between metal electrodes and solar cell active layers. A layer of poly(3,4-ethylenedioxythiophene) (PEDOT) doped with poly(styrene sulfonate) (PSS) has attracted much attention during the last decade.⁹ In typical organic solar cells,^{1,2} the PEDOT:PSS is broadly used to increase the work function of indium-tin oxide (ITO) electrode and to form an ohmic contact between the ITO electrode and the organic active layer. Park *et al.*¹ used a layer of titanium suboxide (TiO_x) as an optical spacer and as a hole blocker between the active layer and the Al electrode; because of the optical spacer, the maximum light intensity was redistributed to be within the active layer, and therefore, the internal quantum efficiency approached 100%. Also, many authors^{10,11} inserted a thin layer of lithium fluoride

(LiF) between metal electrodes and organic active layers for enhancing fill factor and stabilizing high open circuit voltages of the solar cells.

While many aspects of the performance of organic devices are quite well understood, there are properties which are still subject of research worldwide. One of the open issues is the structural and electronic properties of interfaces between the various organic and inorganic components of the devices.¹² Numerous studies have been performed in order to investigate the electronic structure of the organic/metal electrode^{13–15} and organic/organic^{16–18} interfaces, but they are still not completely understood. The understanding of these interfaces is a central issue for the further development of organic solar cells. Although there are several investigations of the properties and electronic structure of organic/metal electrode and organic/organic interfaces, the direct impact of these interfaces on light harvesting and photocurrent of the organic solar cells has not been discussed yet, as far as we know. While the electronic structure of the interfaces, in most previous studies, was one of the main factors determining charge injection conditions and therefore device performance, we surprisingly found that the organic/organic interface had a pronounced impact on the active layer absorption in the visible region of the solar spectrum and therefore on the generated photocurrent from the solar cell.

The beginning of these findings occurred when we spin-coated a blend solution of coumarin 6 dye (C6) and

^{a)}Electronic mail: yasser_ami@yahoo.com.

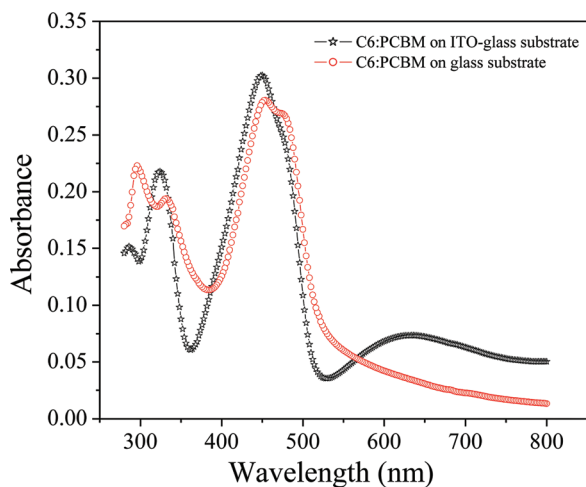


FIG. 1. (Color online) Optical absorbance of C6:PCBM blend films spin-coated onto ITO-glass substrates in comparison with optical absorbance of C6:PCBM blend film spin-coated onto glass substrate.

[6,6]-phenyl- C_{61} butyric acid methyl ester (PCBM) onto clean ITO-glass substrate, as a part of a previous work.¹⁹ After optical absorption measurement of the C6:PCBM blend film, we found an unexpected wide absorption peak at a wavelength of 636 nm, which did not relate $\pi-\pi^*$ transitions of C6 dye or PCBM molecules in the blend.¹⁹ When we spin-coated the same solution with the same conditions onto glass substrate, we did not observe any absorption peaks around the 636 nm, as shown in Fig. 1. The absorption in the wavelength range of 520–800 nm, also, occurred for pristine C6 and pristine PCBM films spin-coated onto clean ITO-glass substrates (not shown here). Thus, the optical absorption in the range of 520–800 nm for the C6, PCBM, and C6:PCBM films does not depend on the type of organic compound in the films. However, what is the cause of the optical absorption at this wavelength range? We try in this paper to answer this question and to illustrate the importance of interfaces between organic layers in the solar cells.

In this paper, we prepare various interfaces (ITO/C6:PCBM, PEDOT:PSS/C6:PCBM, and ITO/PEDOT:PSS/C6:PCBM) to investigate the effect of these interfaces on light harvesting of solar cell active layer and therefore on photocurrent generated by the solar cell. The optical absorption measurement are carried out for C6:PCBM blend film, with different concentrations, spin-coated onto ITO, PEDOT:PSS, and ITO/PEDOT:PSS electrodes. We construct ITO/PEDOT:PSS/C6:PCBM/Al solar cells with varying C6:PCBM blend concentration to investigate the contribution of the C6:PCBM blend films (at the interface with ITO/PEDOT:PSS electrode) to the photocurrent through external quantum efficiency measurement.

II. EXPERIMENTAL PROCEDURES

A. Materials and solutions

The C6 or [3-(2-benzothiazolyl)-7-(diethylamino)coumarin] conjugated dye (99%, Sigma-Aldrich) and PCBM (99.2%, Frontier Carbon Corporation, Japan) were used without further purification. The C6:PCBM blend solutions

with the composition of 40:60 wt. % were prepared by dissolving the two compounds (C6 dye and PCBM) in 1,2-dichlorobenzene (Tokyo Chemical Industry Co. Ltd, Japan) with varying blend concentration as 20, 30, 40, 50, and 60 mg/mL. The solutions were vigorously stirred for more than 24 h at room temperature under nitrogen atmosphere in a glovebox to maximize mixing while avoiding touching the vial cap.

B. Film and device fabrication

The solar cell structure and the fabrication process are almost the same as reported in Ref. 17. The ITO-glass substrates ($\sim 10 \Omega/\square$) were sequentially cleaned in an ultrasonic bath using acetone (twice) and methanol (once), rinsed with de-ionized water, dried inflowing nitrogen, and finally treated by UVO (ultraviolet ozone cleaner) (Filgen, Japan) for more than 1 h. For optical absorption measurement, C6:PCBM blend films with different concentrations were prepared by spin-coating the solutions (1000 rpm) under nitrogen atmosphere in a glove box onto (1) clean ITO-glass substrates, (2) insoluble PEDOT:PSS layer which was spin-coated (2500 rpm) onto clean micro-glass substrates in air, and (3) insoluble PEDOT:PSS layer which was spin-coated onto clean ITO-glass substrates in air. All prepared films were thermally annealed individually using a digitally controlled hotplate at 100 °C for 10 min under nitrogen atmosphere in a glove box. The film preparation and thermal annealing conditions were kept the same as those of the corresponding solar cells for accurate comparison. For solar cell fabrication, an approximately 100-nm-thick Al electrode was thermally deposited onto ITO/PEDOT:PSS/C6:PCBM films using a vacuum deposition system at a pressure of about 3×10^{-4} Pa through a shadow mask to obtain 25 identical cells on one device with an active area of $3 \times 3 \text{ mm}^2$.

C. Measurements

The optical absorption spectroscopy was carried out for ITO/C6:PCBM, PEDOT:PSS/C6:PCBM, and ITO/PEDOT:PSS/C6:PCBM films with varying the C6:PCBM blend concentration using a JASCO V-570 ultraviolet/visible/near-infrared (UV/vis/NIR) spectrophotometer. The external quantum efficiency measurement was performed for ITO/PEDOT:PSS/C6:PCBM/Al solar cells with varying the C6:PCBM blend concentration using a halogen lamp and a monochromator. The J/V characteristics of the devices under white light illumination were determined using standard solar irradiation of 100 mW/cm² (AM1.5) with a JASCO CEP-25BX spectrophotometer J/V measurement setup with a xenon lamp as the light source and a computer-controlled voltage-current source meter (Keithley 238) at 25 °C under nitrogen atmosphere.

III. RESULTS AND DISCUSSION

A. Optical properties of C6:PCBM blend films at different interfaces

Figure 2 shows optical absorption of the C6:PCBM blend films at different concentrations spin-coated onto clean

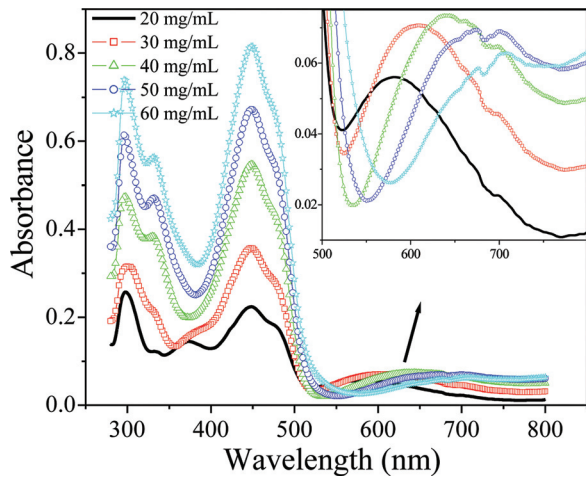


FIG. 2. (Color online) Optical absorbance of C6:PCBM blend films spin-coated onto ITO-glass substrates with variation in C6:PCBM blend concentration. The inset focuses on optical absorbance in the wavelength range of 500–800 nm.

ITO-glass substrates. It is observed from this figure that the fundamental absorption of C6 dye occurs at 450 nm, while the absorption of PCBM molecules occurs around 330 nm. Figure 2 shows an additional absorption area in the spectra at wavelength range of 520–800 nm which is attributed to absorption of the C6:PCBM blend films at the interface with ITO electrode.

The absorption features of the interface become different when the interface structure varies. Figure 3 shows the optical absorption of the C6:PCBM blend films at the interface with PEDOT:PSS layer. The interface here is formed by spin-coating the C6:PCBM blend solutions onto insoluble PEDOT:PSS layer, which was spin-coated in air onto clean microglass substrates.

It is better now to construct and investigate the interface which is presented in an actual working solar cell, i.e., the interface between C6:PCBM blend films and ITO/PEDOT:PSS electrode. This interface is formed by spin-coating C6:PCBM blend solution with different concentrations onto insoluble PEDOT:PSS layer, which was spin-coated in air onto clean

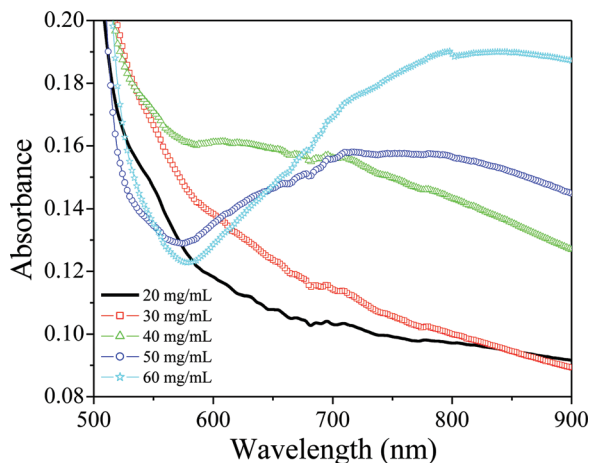


FIG. 3. (Color online) Optical absorbance of C6:PCBM blend films spin-coated onto PEDOT:PSS-micro-glass substrates with variation in C6:PCBM blend concentration.

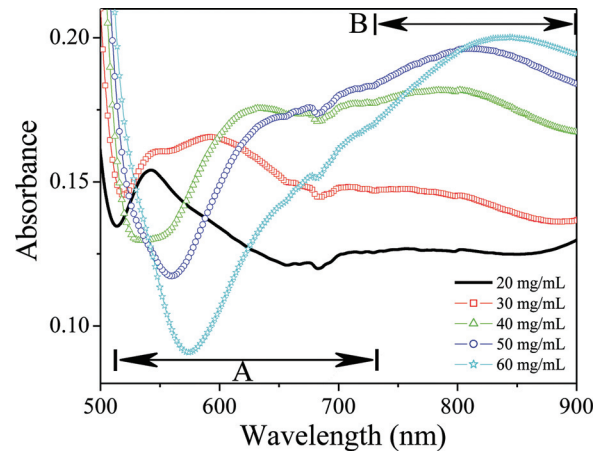


FIG. 4. (Color online) Optical absorbance of C6:PCBM blend films spin-coated onto ITO/PEDOT:PSS-glass substrates with variation in C6:PCBM blend concentration.

ITO-glass substrates. Figure 4 shows optical absorption of the ITO/PEDOT:PSS/C6:PCBM interfaces in the wavelength range of 500–900 nm. As shown in Fig. 4, the ITO/PEDOT:PSS/C6:PCBM interface has two absorption regions; A (in the wavelength range of 520–730 nm) and B (in the wavelength range of 730–900 nm). It is reasonable to consider that, the absorption in region B is due to an interface between C6:PCBM and PEDOT:PSS layers in the ITO/PEDOT:PSS/C6:PCBM films. This is because of the similarity, to a large extent, between the absorption in region B and the absorption of PEDOT:PSS/C6:PCBM interface (shown in Fig. 3), as a result of similarity in the interface structure (PEDOT:PSS/C6:PCBM) in both cases. By comparing between the absorption in region A (shown in Fig. 4) and the absorption of ITO/C6:PCBM interface (shown in Fig. 2), it is reasonable to consider that the absorption in region A resembles, to a large extent, the absorption of ITO/C6:PCBM interface. But, what about a presence of PEDOT:PSS layer between C6:PCBM and ITO layers in the ITO/PEDOT:PSS/C6:PCBM films?

To be able to answer this question we must first understand the nature and origin of the optical absorption of the C6:PCBM blend films at the interfaces with ITO, PEDOT:PSS, and ITO/PEDOT:PSS, electrodes. In the following area of discussion we introduce several facts which may lead to understand the origin of the optical absorption of active layer blend in a favorable wavelength region:

- (1) Optical absorption of the C6:PCBM blend films (as shown in Figs. 2, 3, and 4) occurs in a wavelength range (520–800 nm) at which pristine C6 dye, PCBM, ITO, and PEDOT:PSS films are transparent.
- (2) The absorption in this wavelength range does not relate to a new material other than ITO, PEDOT:PSS, C6, or PCBM, as a result of a chemical interaction between bilayers at the interfaces. For proving this assumption, we spin-coated a layer of C6:PCBM blend onto clean ITO-glass substrate under the same previous conditions. After thermal annealing of the C6:PCBM blend film, we resolved the film by the solution solvent (1,2-dichlorobenzene) and deposited the resulted solution again

two subband transitions (with different optical subband gaps) at the interface with PEDOT:PSS layer. One is due to the charges of PEDOT:PSS semiconductor layer (producing the absorption in region B in Fig. 4), and the other is due to the ITO charges which propagate through the conducting PEDOT:PSS layer (producing the absorption in region A in Fig. 4). As an indication of this discussion, the absorption behavior in region A resembles the absorption behavior shown in Fig. 2, although PEDOT:PSS layer is presented between C6:PCBM blend films and ITO substrate.

The change in the interface structure (ITO/C6:PCBM, PEDOT:PSS/C6:PCBM, or ITO/PEDOT:PSS/C6:PCBM) does not affect the fundamental absorptions of the C6 dye (at 450 nm) or PCBM (at 330 nm) in the blends. However, the change only occurs for absorption of the C6:PCBM blend films beyond the wavelength of 520 nm, as shown in Figs. 2, 3, and 4. As observed from these figures, the absorption peaks in the wavelength range of 520–800 nm increase and shift to higher wavelength, by increasing the C6:PCBM concentration. The increase in absorption peak value may be due to increase in the number of optically induced subband transitions by increasing the film thickness, as a result of increasing blend film concentration. While the redshift in the absorption peak may be due to increase in the interfacial charge carrier concentration (charge density at the interface), which improves the extension of the band tails in the forbidden bandgap of the organic compounds. Therefore, the optical subbandgap varies, and the optical absorption occurs at higher wavelengths.

The absorption of the C6:PCBM blend films at the interface with PEDOT:PSS layer in the ITO/PEDOT:PSS/C6:PCBM films should be taken into account, when someone talks about the importance of light harvesting on the solar cell performance, for two reasons. First, the absorption at the interface occurs at higher wavelengths at which there are the largest numbers of light photons in the solar spectrum. Second, the absorption peaks due to interface reach to pronounced values. For example, the absorption peak value of the C6:PCBM blend film, which has a concentration of 60 mg/mL, reaches to 20% of the incident light, as shown in Fig. 4, while the fundamental absorption peak of the C6 dye in the C6:PCBM blend film, which has a concentration of 20 mg/mL, reaches to 30%.

B. External quantum efficiency spectra

External quantum efficiency (EQE) is defined as the ratio of the number of charges extracted out of the device to the number of incident photons. The EQE spectra of the ITO/PEDOT:PSS/C6:PCBM/Al solar cell with different C6:PCBM blend concentrations are shown in Fig. 6 in the wavelength range from 300 to 800 nm. It is well known that, the photocurrent of a solar cell depends on several factors such as light harvesting, charge carrier separation,²⁴ exciton diffusion, and charge carrier transport.²⁵ The increase in the C6:PCBM blend concentration up to 30 mg/mL increases the active layer thickness, which tends to increase the light harvesting in the solar cell active layer. Consequently, the photocurrent of the solar cell at a wavelength of 455 nm

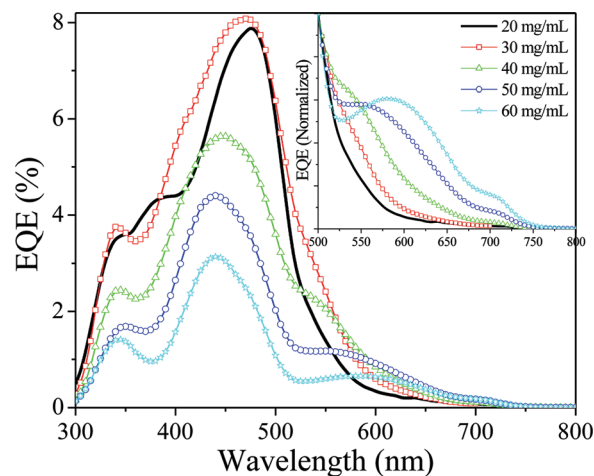


FIG. 6. (Color online) EQE spectra of the ITO/PEDOT:PSS/C6:PCBM/Al solar cells with variation in C6:PCBM blend concentration. The inset shows normalized photocurrent in the wavelength range of 500–800 nm.

increases. While further increase in the active layer thickness by increasing the concentration up to 60 mg/mL reduces the exciton diffusion and/or restricts the mobility of generated charge carriers in the active layer. Therefore, the photocurrent of the solar cell decreases, as shown in Fig. 6.

It is well known that, the EQE spectroscopy is a powerful tool to identify the photoactive materials, which absorb light photons and convert them into charge carriers in the solar cell active layer. The EQE maximum peak of the C6:PCBM active layer around 455 nm (as shown in Fig. 6) relates to the contribution of the C6 dye to the photocurrent, while the dye absorbs light at about 450 nm, as shown in Fig. 2. The EQE spectra in Fig. 6 show the contribution of the PCBM molecules to the photocurrent at a wavelength of approximately 345 nm, while the PCBM absorb light at about 330 nm. It is obvious from Fig. 6 that, there is additional-pronounced photocurrent area in the EQE spectra in the wavelength range of 520–800 nm. Beginning from blend concentration of 30 mg/mL and at the wavelength of 520 nm, a part from EQE spectrum deviates and adopts a different shape, which magnifies and becomes peaklike shape with increasing C6:PCBM blend concentration. Reaching to the concentration of 60 mg/mL, the part of EQE spectrum has a pronounced peak occurring at 580 nm, as shown in the inset of Fig. 6. Particularly at the wavelength range of 600–750 nm and by increasing blend concentration from 20 up to 50 mg/mL, the photocurrent increases and, after that, decreases at the concentration of 60 mg/mL. Thus, the behavior of the photocurrent in this wavelength range is different than the photocurrent in lower wavelengths (300–520 nm, as discussed in the last paragraph). The photocurrent in the wavelength range of 520–800 nm is attributed to optical absorption of the C6:PCBM blend films at the interface with PEDOT:PSS layer. The C6:PCBM blend films form a charge carrier generation interface with PEDOT:PSS layer. At this interface, subband photocurrent is produced as a result of subband transitions, after absorption of light photons by interfacial layer. As an indication of this discussion, one can observe a close relationship and similarity between behavior

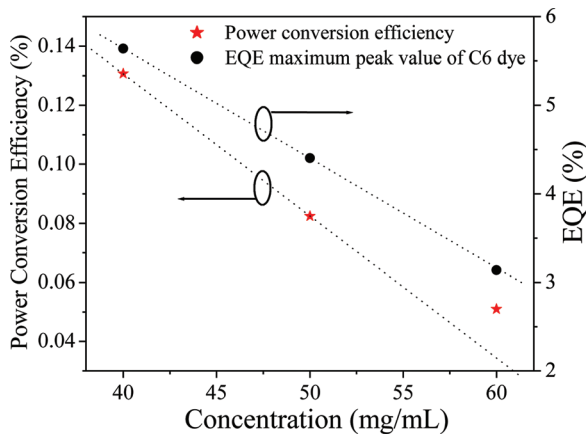


FIG. 7. (Color online) EQE maximum peak value of C6 dye and power conversion efficiency of the ITO/PEDOT:PSS/C6:PCBM/Al solar cells with variation in C6:PCBM blend concentration.

of EQE spectra in the range of 600–750 nm (as shown in Fig. 6) and behavior of optical absorption in region A (as shown in Fig. 4) with increasing C6:PCBM blend concentration. The photocurrent of the interfacial layer is produced as a result of exciton dissociation at the PEDOT:PSS/C6:PCBM interface under the influence of large internal electric field of the charges which are collected at the interface due to connection between C6:PCBM film and ITO/PEDOT:PSS electrode.

The observed photocurrent at higher wavelength reveals a new and important aspect in the photocurrent spectra of the organic solar cells. The importance appears through new information about the electronic interactions at the interface between different layers in the organic solar cells. In addition and most importantly, the observed photocurrent can contribute to improve solar cell performance parameters. This improvement can be illustrated by comparing between the EQE maximum peak value of the C6 dye (extracted from Fig. 6) and the measured power conversion efficiency of the corresponding solar cells, as shown in Fig. 7. In this figure, with varying C6:PCBM blend concentration, the EQE maximum peak value of the C6 dye decreases linearly, while the

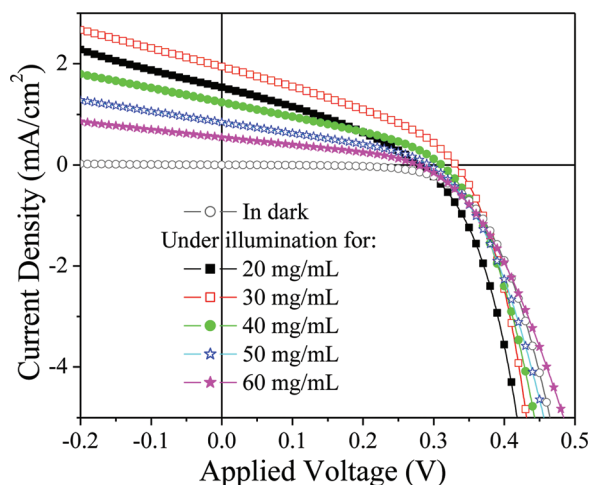


FIG. 8. (Color online) Current density/voltage characteristics in dark and under illumination of the ITO/PEDOT:PSS/C6:PCBM/Al solar cells with variation in C6:PCBM blend concentration.

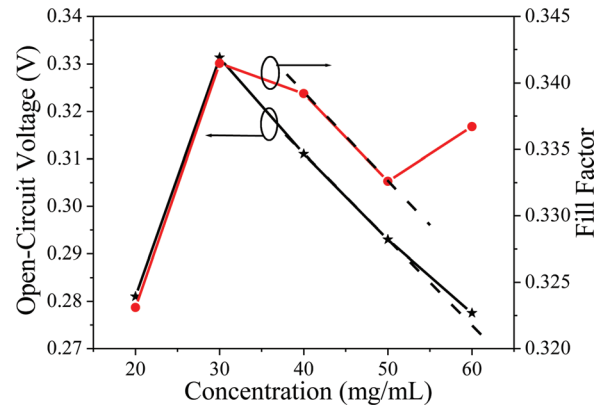


FIG. 9. (Color online) Open-circuit voltage and fill factor vs. C6:PCBM blend concentration of the ITO/PEDOT:PSS/C6:PCBM/Al solar cells.

power conversion efficiency of the corresponding solar cell with the concentration of 60 mg/mL deviates from the expected linearity which occurs for lower concentrations, 40 and 50 mg/mL. Therefore, the efficiency of the solar cell, which has the concentration of 60 mg/mL, is improved, due to the additional photocurrent of the C6:PCBM blend film at the interface with PEDOT:PSS layer. The power conversion efficiency of the solar cells is obtained from the analysis of the J/V characteristics of the solar cells at different C6:PCBM blend concentrations, as shown in Fig. 8. Relying on Fig. 8, the device performance parameters (short-circuit current density, open-circuit voltage, and fill factor) can be obtained. Figures 9 and 10 show the variation of these parameters with C6:PCBM blend concentration in the solar cell. From these figures especially for the solar cell which has 60 mg/mL as an active layer concentration, we can observe deviation of all performance parameters from the linearity, which occurs at lower concentrations of the solar cell active layer. The deviations of short-circuit current density and open-circuit voltage shown in these figures are rather small, while only fill factor exhibits a clear and large deviation from a linear behavior at higher C6:PCBM blend concentration. Relying on the fact that fill factor depends on series resistance in the solar cell, we may assume that the

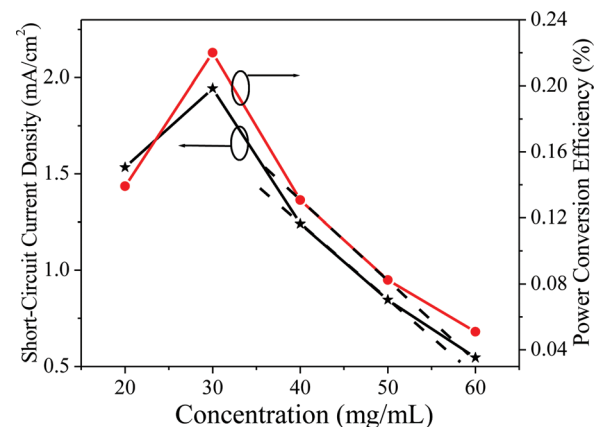


FIG. 10. (Color online) Short-circuit current density and power conversion efficiency vs. C6:PCBM blend concentration of the ITO/PEDOT:PSS/C6:PCBM/Al solar cells.

clear and large deviation in the fill factor at higher C6:PCBM concentration (as shown in Fig. 9) may be due to increase in the charge carrier concentration (at the interface), which improves the extension of the band tails and, therefore, modifies energy situation for charge transfer at the interface, as show in Fig. 5. In this case, the holes from HOMO of the C6 move easily into HOMO of the PEDOT:PSS, and therefore the series resistance decreases, and the fill factor clearly increases. These observations represent further indication of that, the subband absorption and therefore the photocurrent at organic/organic interface may improve power conversion efficiency of the organic solar cells. The observed improvement in power conversion efficiency of the solar cell is small, but it is a strong indication of presence and importance of the organic/organic interface. The contribution of the organic/organic interface to the photocurrent still needs excess of experiments for improvement and to become more effective for solar cell performance. When the photocurrent of interfacial layer becomes effective for solar cell performance, the current considerations to high-band-gap donor materials will change. We hope to do that in the near future.

IV. CONCLUSIONS

This work represents the first findings, as far as we know, which illustrate the importance of the interface between solar cell active layer and ITO/PEDOT:PSS common electrode. In this work, the optical absorption measurement was carried out for C6:PCBM blend film with different concentrations spin-coated onto clean ITO, insoluble PEDOT:PSS, and insoluble ITO/PEDOT:PSS electrodes, for comparison. We found an additional absorption region in the optical spectra of the C6:PCBM blend films at the wavelength range of 520–800 nm, at which the C6 dye, PCBM, PEDOT:PSS, and ITO were transparent. The difference in the absorption spectra in this wavelength range depended on difference in the interface structure, i.e., ITO/C6:PCBM, PEDOT:PSS/C6:PCBM, and ITO/PEDOT:PSS/C6:PCBM. By increasing the C6:PCBM blend concentration for different interface structures, the absorption peaks in the wavelength range of 520–800 nm increased and shifted to higher wavelength. The effect of optical absorption on the photocurrent of the C6:PCBM blend films (at the interface with ITO/PEDOT:PSS electrode) was studied through the construction of ITO/PEDOT:PSS/C6:PCBM/Al solar cells with varying C6:PCBM blend concentration and through the measurement of external quantum efficiency of these solar cells. In external quantum efficiency spectra, we found an additional contribution to the photocurrent in the wavelength range of 520–800 nm due to the interface between C6:PCBM blend films and ITO/PEDOT:PSS electrode. Due to the photocurrent contribution of the interfacial layer, the power conversion efficiency of the corresponding solar cell was improved. The new features in the optical absorption and photocurrent spectra of the investigated solar cells originated, in all probabilit-

ity, due to optically induced subband transitions in the C6:PCBM blend films at the interface with ITO/PEDOT:PSS electrode. So, the increase and redshift of the absorption peaks, with increasing C6:PCBM blend concentration, were attributed to the increase in the number of optically induced subband transitions and the increase in the interfacial charge carrier concentration, respectively. By considering these new findings, the high-band-gap organic materials will take more importance as sensitizers in organic optoelectronic applications.

ACKNOWLEDGMENTS

Yasser A. M. Ismail acknowledges the Egyptian people and government for financial supporting of this work.

- ¹S. H. Park, A. Roy, S. Beaupré, S. Cho, N. Coates, J. S. Moon, D. Moses, M. Leclerc, K. Lee, and A. J. Heeger, *Nat. Photonics* **3**, 297 (2009).
- ²H.-Y. Chen, J. Hou, S. Zhang, Y. Liang, G. Yang, Y. Yang, L. Yu, Y. Wu, and G. Li, *Nat. Photonics* **3**, 649 (2009).
- ³Y. Y. Liang, Y. Wu, D. Feng, S.-T. Tsai, H.-J. Son, G. Li, and L. Yu, *J. Am. Chem. Soc.* **131**, 56 (2009).
- ⁴N. Blouin, A. Michaud, and M. Leclerc, *Adv. Mater.* **19**, 2295 (2007).
- ⁵F. Banishoeib, A. Henckens, S. Fourier, G. Vanhooyland, M. Breselge, J. Manca, T. J. Cleij, L. Lutsen, D. Vanderzande, L. H. Nguyen, H. Neugebauer, and N. S. Sariciftci, *Thin Solid Films* **516**, 3978 (2008).
- ⁶Y. A. M. Ismail, T. Soga, and T. Jimbo, *Sol. Energy Mater. Sol. Cells* **94**, 1406 (2010).
- ⁷Y. A. M. Ismail, T. Soga, and T. Jimbo, *Sol. Energy Mater. Sol. Cells* **93**, 1582 (2009).
- ⁸J. Y. Kim, S. H. Kim, H. Lee, K. Lee, W. Ma, X. Gong, and A. J. Heeger, *Adv. Mater.* **18**, 572 (2006).
- ⁹L. Groenendaal, F. Jonas, D. Freitag, H. Pielartzik, and J. R. Reynolds, *Adv. Mater.* **12**, 481 (2000).
- ¹⁰C. J. Brabec, S. E. Shaheen, C. Winder, N. S. Sariciftci, and P. Denk, *Appl. Phys. Lett.* **80**, 1288 (2002).
- ¹¹L. J. A. Koster, V. D. Mihailetschi, H. Xie, and P. W. M. Blom, *Appl. Phys. Lett.* **87**, 203502 (2005).
- ¹²W. Brütting, *Physics of Organic Semiconductors* (Wiley, New York, 2005).
- ¹³H. Peisert, T. Schwieger, M. Knupfer, M. S. Golden, and J. Fink, *J. Appl. Phys.* **88**, 1535 (2000).
- ¹⁴I. G. Hill, A. J. Mäkinen, and Z. H. Kafafi, *Appl. Phys. Lett.* **77**, 1825 (2000).
- ¹⁵V. Papaefthimiou and S. Kennou, *Surf. Sci.* **566**, 497 (2004).
- ¹⁶H. Peisert, M. Knupfer, F. Zhang, A. Petr, L. Dunsch, and J. Fink, *Appl. Phys. Lett.* **83**, 3930 (2003).
- ¹⁷S. Braun, M. P. de Jong, W. Osikowicz, and W. R. Salaneck, *Appl. Phys. Lett.* **91**, 202108 (2007).
- ¹⁸Y.-K. Kim, J. W. Kim, and Y. Park, *Appl. Phys. Lett.* **94**, 063305 (2009).
- ¹⁹Y. A. M. Ismail, T. Soga, and T. Jimbo, *Jpn. J. Appl. Phys.* **49**, 052301 (2010).
- ²⁰A. A. Bakulin, S. G. Elizarov, A. N. Khodarev, D. S. Martyanov, I. V. Golovnin, D. Y. Paraschuk, M. M. Triebel, I. V. Tolstov, E. L. Frankevich, S. A. Arnautov, and E. M. Nechvolodova, *Synth. Met.* **147**, 221 (2004).
- ²¹A. A. Bakulin, D. S. Martyanov, D. Yu. Paraschuk, M. S. Pshenichnikov, and P. H. M. van Loosdrecht, *J. Phys. Chem. B* **112**, 13730 (2008).
- ²²J. D. Dow and D. Redfield, *Phys. Rev. B* **5**, 594 (1972).
- ²³M. Ohtomo, T. Shimada, K. Saiki, and T. Hasegawa, *J. Appl. Phys.* **102**, 064510 (2007).
- ²⁴Y. Kim, S. A. Choulis, J. Nelson, D. D. C. Bradley, S. Cook, and J. R. Durrant, *J. Mater. Sci.* **40**, 1371 (2005).
- ²⁵T. Yohannes, F. Zhang, M. Svensson, J. C. Hummelen, M. R. Andersson, and O. Inganäs, *Thin Solid Films* **449**, 152 (2004).